Journal of Thermal Analysis, Vol. 5 (1973) 19—32

THERMAL REACTIONS OF INORGANIC HYDROXY-COMPOUNDS UNDER APPLIED ELECTRIC FIELDS, II

DEHYDROXYLATION OF $Mg(OH)_2$ and $Al(OH)_3$

K. J. D. MACKENZIE*

Department of Ceramics, University of Sheffield, Sheffield, England

(Received March 18, 1971; in revised form November 9, 1971)

The effect of electric fields on the thermal dehydroxylation of $Mg(OH)_2$ (brucite) and $Al(OH)_3$ (gibbsite) have been studied by thermogravimetry in a controlled inert atmosphere. Electric fields exert no beneficial effect on the reaction of gibbsite; in some cases the reaction is slightly retarded. By contrast, a small but significant beneficial effect is observed in brucite, in which the initiation temperature and activation energy is lowered at field strengths of about 10^5 V/m. The difference in behaviour of the two hydroxides is attributed to differences in the mobility of anionic defects and oxygen-containing "proton-transfer complexes". The transport of the various proton-bearing species in an electric field is discussed.

In a previous paper [1] it was shown that the application of an electric field to the hydroxy-aluminosilicate kaolinite [$Al_2Si_2O_5(OH)_4$] during dehydroxylation resulted in a decreased activation energy for the process, the effect of the field being most pronounced at lower temperatures. Since at higher temperatures the reaction in kaolinite is apparently dominated by defect formation, on which the field exerts less effect, it is interesting to study the influence of electric fields on the dehydroxylation of related simple hydroxides such as $Mg(OH)_2$ and $Al(OH)_3$, which represent opposite extremes of proton retention behaviour. In the former material, and in related magnesium hydroxy-minerals generally, the dehydroxylation temperature is higher than in the aluminium analogues but crystalline products are formed immediately on dehydroxylation, by contrast with the aluminium compounds, which form a wide range of less crystalline intermediates [2]. This behavioural difference between magnesium and aluminium compounds has been explained [3] in terms of facilitation of ionic migration in the former by relatively more mobile and less tightly bound protons (as in an inhomogeneous mechanism [4]). Another suggestion [4] is that the elements of water are removed with equal facility from both types of hydroxide, but in the aluminium compounds the comparative lack of mobility of dislocations and defects hinders the changes in oxygen packing necessary for the formation of new compounds. Since the application of an electric field influences both proton migration and to a lesser extent defect movement [1] the present electrolysis studies should also provide information on the relative importance of both processes in these compounds.

* Present address: Chemistry Division, D.S.I.R., Gracefield, Wellington, New Zealand.

As in the previous work on kaolinite [1], TG kinetic measurements were made solely as a means of comparison between electrolysed and unelectrolysed samples. No mechanistic comparison was attempted between the present work on $Mg(OH)_2$ and the results of previous workers [5–8] although the inhomogeneous mechanism of Ball and Taylor [9] has provided a basis for understanding the electrolysis results, despite the fact that some of the X-ray evidence for this mechanism [9] has now been discounted [10].

The extraction of meaningful kinetic data from weight-loss measurements of aluminium hydroxide is even more difficult because of the existence of three forms of $Al(OH)_3$, viz., gibbsite, bayerite and norstrandite, which can also coexist with two oxyhydroxides, boehmite and diaspore; all these are thermally decomposed to corundum (α-Al_2O_3) via different sequences of intermediates. The decomposition sequences can also be modified by the physical sample conditions – small crystals of gibbsite decompose via two intermediates whereas larger crystals initially form some boehmite which decomposes via different intermediates [11]. Previous kinetic studies of gibbsite dehydroxylation [12, 13] have also shown that the activation energy is sensitive to the partial pressure of water vapour present [12] in a similar manner to kaolinite [14].

Kinetic studies of these materials are therefore useful for comparison purposes only when the same materials are reacted under conditions as identical as experimentally possible; strict precautions were taken in the present work to meet this criterion. Additional information about the electrolysis process was sought by X-ray examination of the solid reaction product, and in the case of $Mg(OH)_2$ by X-ray line broadening measurements of the crystallite size of the product.

Experimental

a) Materials

Pure $Mg(OH)_2$ was prepared by steaming high purity magnesium turnings with distilled water in a pressure vessel lined with fused silica. The X-ray trace of the product showed it to be well crystallized brucite [$Mg(OH)_2$].

The synthetic gibbsite sample was obtained from the OECD Mineral Bank and has been fully characterized by that organisation. The X-ray trace shows this material to be well crystallized gibbsite with no abnormalities but the DTA and DTG traces (Fig. 1) show three peaks, at 230, 320 and 580°, corresponding respectively to the formation of some boehmite, dehydroxylation of the remaining gibbsite and dehydroxylation of the boehmite [11]. This behaviour is typical of a sample of large crystallite size [11].

Pellets of $Mg(OH)_2$ and $Al(OH)_3$ were prepared by pressing 0.5 g powder samples in a 1.1 cm dia. stainless steel die at 560 kg/cm^2. Since the dehydroxylation kinetics were expected to be influenced by the degree of sample compaction, the bulk density of each pellet was measured by the mercury method of Clark and White [15] to select for the kinetic measurements those pellets having densities differing by not more than ± 0.001 g/cc.

b) Electrolysis experiments

Weight-loss measurements were made using the electrolysis cell previously described [1] in conjunction with a Stanton TR – 1 thermobalance. The samples were heated at a linear temperature rise of 2°/min. in a flowing atmosphere of dried argon (300 ml/min.). The electrolysing potential [600 V, 8 mA for $Mg(OH)_2$, 400 V, 8 mA for $Al(OH)_3$] was started at room temperature in some experiments and at dehydroxylation temperatures [300° for $Mg(OH)_2$, 220° for $Al(OH)_3$] in other experiments. The electrical polarity was reversed with respect to the gas flow in some runs and control experiments with unelectrolysed pellets and powders were also made.

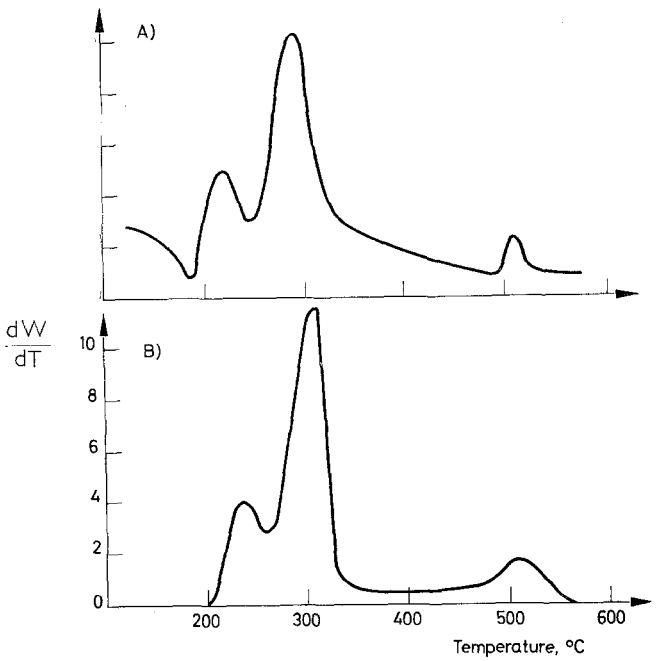

Fig. 1. A. DTA trace of O.E.C.D. gibbsite, $Al(OH)_3$. B. DTG trace of O.E.C.D. gibbsite, $Al(OH)_3$

In the case of $Al(OH)_3$, the initial formation of some boehmite (Fig. 1) presents difficulties since the kinetic measurements must be made on one reaction alone, viz. the dehydroxylation of gibbsite. The problem was overcome by holding the gibbsite samples at 220° at the start of a run until the boehmite-forming reaction was complete and constant weight obtained. The dynamic weight-loss measurements were then started and the dehydroxylation of gibbsite allowed to proceed to completion.

c) X-ray examination of the products

Both faces of each pellet were examined after reaction by X-ray diffractometry using a Philips goniometer and Cu Kα radiation. The crystallite size of MgO was also estimated from line-width measurements made on the major oxide peak at 42.82° 2Θ at a scan speed of $^1/_4$° 2Θ/min.

Results

a) $Mg(OH)_2$

Plots of the degree of dehydroxylation (α) as a function of temperature are given in Fig. 2, showing that the application of an electric field decreases the reaction temperature and is independent of the direction of gas flow. The reaction temperature is initially lower in samples electrolysed while being heated to dehydroxylation temperature, but all the curves converge after about 40% reaction. Although not relevant to the electrolysis data which were obtained for pellets, the results obtained for an unelectrolysed powder are included for interest in Fig. 2. The reaction temperature for a powder is much lower than for an unelectrolysed pellet, from which the escape of water is more difficult.

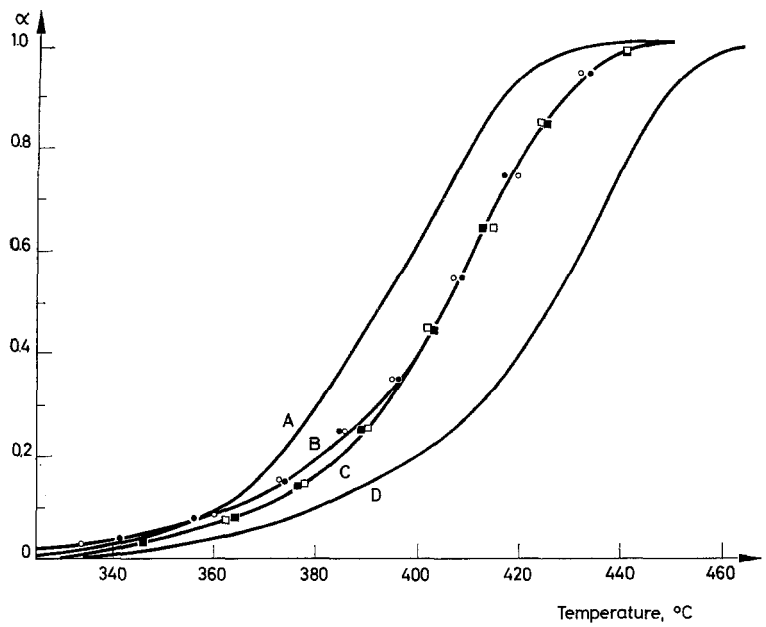

Fig. 2. Graphs of fraction $Mg(OH)_2$ reacted as a function of temperature. Description of samples A to D as given in Table 1. ■, ● gasflow −ve to +ve. □, ○ gas flow +ve to −ve

The weight-loss data were analysed in terms of the Coats and Redfern equation using a computer programme as previously described [1]. The best linear fit of the data was given by a first-order rate law from which activation energies and pre-exponential factors were calculated (Table 1). The reproducibility of the

Table 1

Kinetic parameters derived from a first-order model and X-ray crystallite size determinations for electrolysed and unelectrolysed $Mg(OH)_2$ samples

Sample geometry	Reaction conditions	Direction of gas flow	Activation energy ΔH^*, kcal/mole	Pre-exponential factor, A	X-ray crystallite size, Å +ve face	X-ray crystallite size, Å −ve face
Pellet C*	600 V applied at 20°	−ve to +ve	34.8	2.29×10^{8}	102	109
Pellet B	600 V applied at 300°	−ve to +ve	37.8	8.32×10^{6}	103	117
Pellet C	600 V applied at 20°	+ve to −ve	37.8	1.41×10^{7}	108	97
Pellet B	600 V applied at 300°	+ve to −ve	37.8	2.63×10^{7}	115	104
Pellet	Unelectrolysed, in cell	—	45.5	2.51×10^{8}	95, 97	
Pellet D	Unelectrolysed, in crucible	—	39.4	1.86×10^{6}	85, 82	
Powder A	Unelectrolysed, in crucible	—	47.8	5.49×10^{9}	86	

* Letters refer to kinetic curves of Fig. 2.

activation energy values was within 0.6 kcal/mole. As in the study of kaolinite [1], no mechanistic significance should be placed on the apparent operation of a first-order law since in some cases almost as good a linear fit of data was given by a two-dimensional advancing interface model ($n = 0.5$). Table 1 shows that the

Table 2

Average values of first-order rate constants for electrolysed and unelectrolysed $Mg(OH)_2$ pellets

Temperature, °C	k_1 (electrolysed), min^{-1}	k_1 (unelectrolysed), min^{-1}
337	6.92×10^{-8}	6.17×10^{-8}
360	2.04×10^{-7}	2.45×10^{-7}
377	4.57×10^{-7}	6.64×10^{-7}
393	9.55×10^{-7}	1.51×10^{-6}
431	4.47×10^{-6}	9.77×10^{-6}

activation energy for all the electrolysed samples is decreased by an average of 6.2 kcal/mole, comparable with the decrease observed in electrolysed kaolinite [1]. Although comparisons of activation energies obtained under differing experimental conditions are not very meaningful, the present activation energies are of the order of those obtained by Gordon and Kingery for polycrystalline brucite [5] and by Turner et al. for powder samples [8] but are at variance with other reported values [6, 7]. The pre-exponential factors (Table 1) are virtually unaffected by the field, there being a large error in the graphical determination of this parameter.

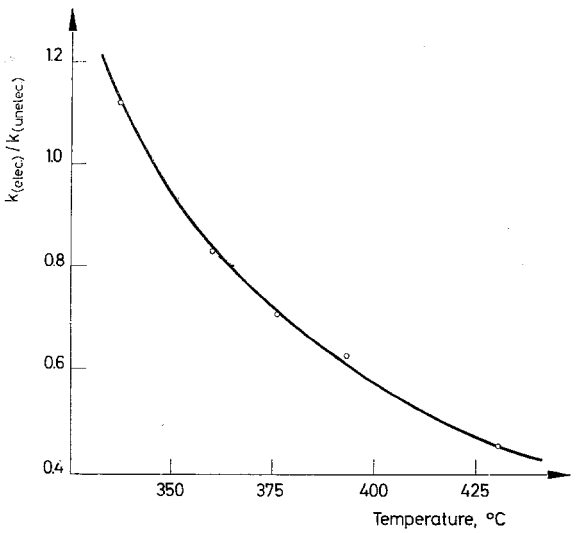

Fig. 3. Plot of ratio of first-order rate constants for electrolysed and unelectrolysed $Mg(OH)_2$ pellets as a function of temperature

Mean values of the first-order rate constants for electrolysed and unelectrolysed pellet samples are given in Table 2, showing that although at lower temperatures the rate is slightly increased by the field, a progressive decrease in rate is observed at higher temperatures. The plot of k_1(electrolysed)/k_1(unelectrolysed) vs. temperature (Fig. 3) is of similar form to that observed for kaolinite [1], in which however the ratio was always >1 over the temperature range of dehydroxylation.

The crystallite size D of the oxide at both faces of each reacted pellet was calculated from the X-ray line width measurements by the relationship

$$D = K\lambda/\beta \cos \Theta \qquad (1)$$

where λ is the wavelength of the X-rays, Θ is half the diffraction angle 2Θ in radians, β is the pure diffraction breadth of the X-ray line profile at half intensity and K is a constant depending on the particle shape and mode of definition of D and β.

A value of $K \approx 1$ has been found to give reasonable results for MgO [16] when D is defined as (volume of crystallites)$^{1/3}$. The measured values of profile linewidths were corrected for instrumental broadening by assuming Gaussian profiles and applying the Warren correction [16]. Corrections were also made for broadening due to the $\alpha_1\alpha_2$ doublet by the graphical method of Jones [17].

The values for crystallite sizes given in Table 1 show that electrolysis produces a consistent increase of up to 43% in the crystallite size of the product oxide, the effect being in each case most marked at the pellet face nearest the incoming gas flow. A similar trend was not recorded in the unelectrolysed pellets, suggesting that the effect is due to a combination of electrolysis and removal of the gaseous products. The differences in crystallite size in the electrolysed samples are real, being much greater than the differences in the unelectrolysed samples which are of the order of the reproducibility of these measurements.

b) $Al(OH)_3$ (gibbsite)

Plot of α as a function of temperature (Fig. 4) shows that by contrast with $Mg(OH)_2$ and kaolinite [1], the reaction temperature is in every case *increased* by the application of a field, the greatest increase occurring for samples electrolysed during heating.

Analysis of the weight-loss data by the Coats and Redfern equation showed that the best linear fit of the data was given by a two-dimensional interface model ($n = 0.5$). The activation energies and pre-exponential factors calculated from this model are given in Table 3, and apparently follow no particular trend, being

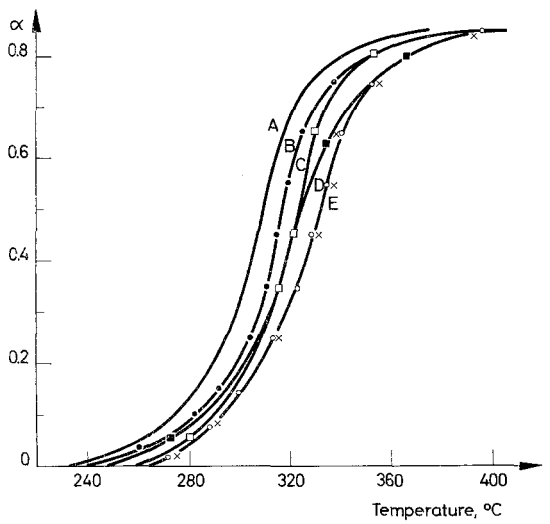

Fig. 4. Graphs of fraction $Al(OH)_3$ (gibbsite) reacted as a function of temperature. Description of samples A to E as given in Table 3. ○, ■ gas flow −ve to +ve. □, × gas flow +ve to −ve

Table 3

Kinetic parameters derived from a two-dimensional interface model for electrolysed and unelectrolysed $Al(OH)_3$ (gibbsite) samples

Sample geometry	Reaction conditions	Direction of gas flow	Activation energy ΔH^*, kcal/mole	Pre-exponential factor, A
Pellet E*	400 V applied at 20°	−ve to +ve	30.6	8.51×10^{4}
Pellet D	400 V applied at 220°	−ve to +ve	32.8	2.09×10^{6}
Pellet E	400 V applied at 20°	+ve to −ve	27.2	7.94×10^{3}
Pellet C	400 V applied at 220°	+ve to −ve	27.6	2.14×10^{4}
Pellet B	Unelectrolysed, in cell	—	28.5	5.37×10^{4}
Pellet B	Unelectrolysed, in crucible	—	28.0	1.85×10^{5}
Powder A	Unelectrolysed, in crucible	—	30.0	4.36×10^{5}

* Letters refer to the kinetic curves of Fig. 4.

scattered about the measured parameters of the unelectrolysed control samples. The reproducibility of the activation energies was within 0.5 kcal/mole. Table 3 also shows that the dehydroxylation of gibbsite is much more sensitive to the reaction atmosphere than either $Mg(OH)_2$ or kaolinite, the activation energy of gibbsite being dependent on the direction of gas flow with respect to the electrolysing voltage. As in the case of $Mg(OH)_2$, the pre-exponential factors are apparently insensitive to the field.

As far as a comparison is meaningful, all the activation energies are of the order of those previously reported [12, 13], which were however derived in a different manner. Mean values of the electrolysed and unelectrolysed rate constants are given in Table 4, showing that at all temperatures the electric field retards the reaction, particularly so at higher temperatures (Fig. 5).

Table 4

Average values of two-dimensional interface rate constants for electrolysed and unelectrolysed $Al(OH)_3$ (gibbsite) pellets

Temperature, °C	k (electrolysed), min^{-1}	k (unelectrolysed) min^{-1}
265	7.08×10^{-8}	8.13×10^{-8}
276	1.70×10^{-7}	2.14×10^{-7}
295	4.07×10^{-7}	5.62×10^{-7}
315	9.77×10^{-7}	1.48×10^{-6}
344	3.16×10^{-6}	4.68×10^{-6}

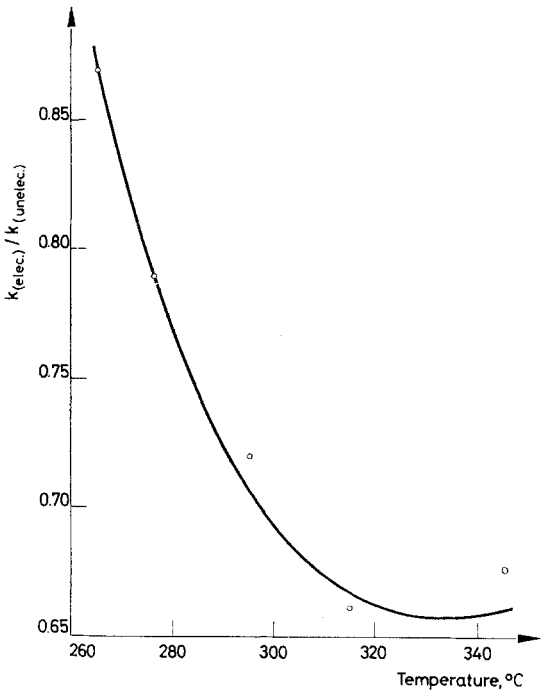

Fig. 5. Plot of ratio of two-dimensional interface rate constants for electrolysed and unelectrolysed $Al(OH)_3$ (gibbsite) pellets as a function of temperature

X-ray examination of the final products showed these to possess typically diffuse patterns in all cases, with no differences in phase or crystallinity detectable between the positive and negative electrode faces of any of the electrolysed pellets. The observed lattice spacings corresponded closely with those of ψ-alumina given by Brindley and Choe [11], with the exception of one peak at about 2.28 Å, which is however ascribed to ψ-alumina by Russell et al. [18].

Discussion

The most striking feature of these results is the difference between the dehydroxylation behaviour of $Mg(OH)_2$ and $Al(OH)_3$ under an electric field. Since both $Mg(OH)_2$ and $Al(OH)_3$ have been said to retain protons during dehydroxylation and to lose water by a mechanism involving the tunnelling of these protons through the P.E. barrier [19], the effect of the field on the protons should be similar in both materials. The tunnelling probability of the proton depends on the height and width of the energy barrier which in turn depends on the dissociation energy of the O–H bond in the crystalline hydroxide; this energy has been cal-

culated for crystalline $Mg(OH)_2$ and $Al(OH)_3$ (gibbsite) [20] as -120.5 and -115.3 kcal/mole respectively. The proton transfer properties should therefore be very similar in both materials, and although protons are the major current carriers at lower temperatures, the observed differences in electrolysis behaviour cannot be explained in terms of differences in tunnelling.

As well as involving migration of protons, the transformation of hydroxide to oxide is accompanied by changes in oxygen configuration. In $Mg(OH)_2$ the transformation is facile and probably occurs by movement of dislocations [4]; the hexagonal close packed oxygen atoms of the hydroxide become cubic close packed in the oxide with the (111) and $(1\bar{1}0)$ planes perpendicular to the *c* and *a* axes of the hydroxide [9]. In gibbsite a series of hexagonal intermediate phases is formed on initial dehydroxylation, either because of difficulty in cation migration due to proton retention [3] or difficulty in anion rearrangement due to immobility of defects [4]. If, as has been recently suggested [21], the long-range movement of protons depends on the migration of oxygen-containing "transport complexes" such as H_2O^+, the electrolytic weight-loss behaviour of these hydroxides should reflect their oxide ion behaviour. Since the movement of oxide ions in $Mg(OH)_2$ is facile, migration of charged oxygen-containing "transport complexes" should likewise be facile, with a consequent enhancement of long-range proton migration, as is shown by the positive effect of electric fields on dehydroxylation of $Mg(OH)_2$ at lower temperatures. That a mass transfer process is apparently operating in $Mg(OH)_2$ is also borne out by the observed differences in the crystallite sizes at opposite ends of the electrolysed pellets (Table 1). The interpretation of these results is, however, complicated by the presence of water vapour concentration gradients at that end of the pellet nearest the incoming gas stream; water vapour is known to markedly assist nucleation and crystal growth in MgO [22] making it difficult to tell in the present case whether the increase in crystallite size is mainly due to the transfer of oxygen-containing complexes and/or Mg^{2+} ions to one end of the pellet or to the build-up of water vapour at one electrode by electrolysis of protons.

In the case of gibbsite the negative effect of the field suggests that the preferred formation of intermediate phases is not wholly due to proton retention since despite a greater cation-proton affinity the application of a field should lead to enhanced proton elimination at lower temperatures. If, however, the long-range migration of protons depends on a relatively slow oxygen-complex transport mechanism which is much less affected by the field than is proton tunnelling, neither the formation of new phases nor the elimination of water will be enhanced by electrolysis, as is experimentally the case. Therefore although the mechanism of proton elimination from gibbsite is similar to that of $Mg(OH)_2$ and kaolinite its anomalous electrolysis behaviour is due to a factor which is relatively uninfluenced by the field. There is, however, evidence that at higher temperatures at which the mobility of the oxygen atoms is improved, the formation of the final product (α-alumina) is enhanced by an electric field (K. J. D. MacKenzie, unpublished results).

Transfer probabilities of proton-bearing complexes in an electric field

Since the foregoing discussion turns on the comparative effect of a field on the mobilities of protons and oxygen-containing "transport complexes" it is now of interest to consider in more detail the transfer probability of these species.

The tunnelling probability P_w of a proton in an unperturbed boehmite lattice has already been calculated [20] by adapting an equation given by Eckart [23] for the penetration of a potential barrier by electrons:

$$P_w = \frac{\cosh 4\pi\beta - 1}{\cosh 4\pi\beta + \cosh 2\pi\delta} \tag{2}$$

where

$$\beta = \frac{l_0}{h}(2mW^*)^{\frac{1}{2}} \tag{3}$$

and

$$\delta = \frac{1}{2}\left(\frac{32E^* ml_0^2}{h^2} - 1\right)^{\frac{1}{2}} \tag{4}$$

In these equations, m is the mass of the tunnelling particle of energy W^* and E^* and l_0 is the barrier height and width respectively. To estimate E^* and l_0 it is necessary to assume a potential function for the energy well in the direction of the tunnelling axis. In previous calculations for boehmite [20] this was taken as a Morse function but values of $(E^* - W^*)$ were mistakenly substituted for E^* [24], leading to the conclusion that the tunnelling probability P_w approaches unity at an energy level of about 11 kcal above the fundamental. Calculations made with correct values of E^* show that the tunnelling probability of the proton follows a similar curve to that previously published [20] (Fig. 6A) but the probability approaches unity at higher energy levels, viz. 28 – 29 kcal. Since the dissociation energies of O – H are not significantly different in boehmite, gibbsite or brucite [20], similar results would be expected for proton tunnelling in all these materials.

In the presence of an electric field, the P.E. barrier will be distorted, making it necessary to define a new barrier shape in order to calculate the effect of the field on P_w. To establish the shape of the distorted barrier it is necessary to define the wave function of the double minimum potential and perturb this function by a term involving the electric field. This treatment will be published in Part III. If, however, it is assumed that the barrier to proton tunnelling is reduced by approximately the same amount as observed in $Mg(OH)_2$ the effect on tunnelling probability can be calculated. Fig. 6B shows that the probability function has the same shape in both cases but the curves are displaced to lower energies by reducing the barrier height. The curve shapes are insensitive to quite large variations in barrier width.

Similar calculations of tunnelling probability can be made for more massive species such as the "transport complex" but in doing so it must be remembered that the concept of tunnelling and its wave-mechanical treatment is strictly only

applicable to very light, energetic species to which can be ascribed wave properties. The effect of increasing the mass of the tunnelling species 18-fold (i.e. corresponding to the species H_2O^+) is shown in Fig. 6C. For the purpose of this calculation an energy barrier of the order of the dehydroxylation energy has been assumed. Fig. 6C shows that the shape of this curve is quite different from that for proton

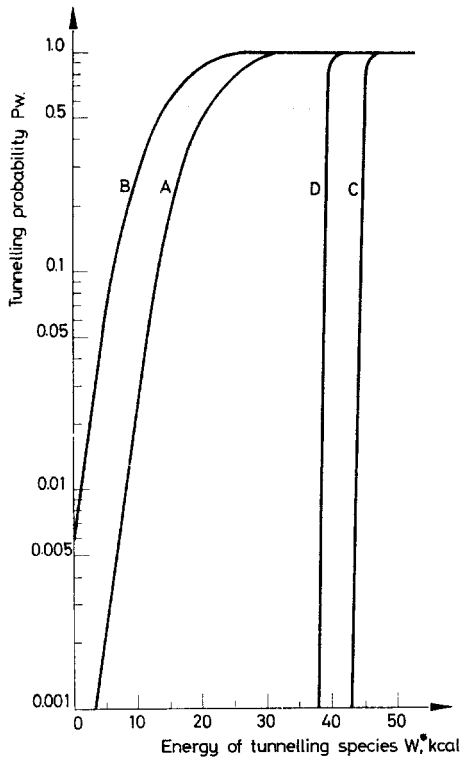

Fig. 6. Tunnelling probability P_w of various species as a function of their energy W^*. A. Proton at an energy barrier of 21.2 kcal. B. Proton at an energy barrier of 15.0 kcal. C. Species of mass 18 (H_2O^+) at an energy barrier of 45 kcal. D. Species of mass 18 (H_2O^+) at an energy barrier of 39 kcal

tunnelling and predicts negligible transfer until the barrier height is exceeded by the energy of the charged species, at which stage a transfer process not involving tunnelling is more likely. Lowering the energy barrier by about 6 kcal (Fig. 6D) again causes displacement of the probability curve without change of shape. The results of Fig. 6, although derived without a precise knowledge of the effect of the field on the energy barrier shape, suggest that short-range proton migration by tunnelling is likely to be assisted by the field whereas the long-range movement of "transport complexes" is virtually unaffected until the energy barrier is exceeded.

In a material such as dehydroxylated gibbsite containing defects of low mobility the field will only become effective when the mobility of all species is increased (at much higher temperatures). Electric fields exert a greater effect on $Mg(OH)_2$ since the oxide ions and defects are apparently sufficiently mobile to allow proton transfer via "transport complexes" as well as by direct tunnelling at lower temperatures.

Conclusions

The application of an electric field to $Mg(OH)_2$ during dehydroxylation produces an increase in the reaction rate at lower temperatures by enhancing proton tunnelling. The increase in rate falls off at higher temperatures as the mechanism changes to one involving proton transfer via a "transport complex" on which the field has less effect. The increase in crystallite size recorded at the pellet face nearest the incoming gas flow may be due to water vapour concentration gradients in the sample.

By contrast, the electric field has a slightly retarding effect on the dehydroxylation of $Al(OH)_3$, possibly due at lower temperatures to a greater affinity between the cation and the proton but due at higher temperatures to the lack of mobility of the oxide ions and the oxygen-containing "transport complex".

*

This work was carried out under an S.R.C. research grant. The helpful discussion of Dr W. T. Raines and communications from Dr P. G. Rouxhet are appreciated.

References

1. K. J. D. MacKenzie, J. Thermal Anal., 5 (1973) 5.
2. N. H. Brett, K. J. D. MacKenzie and J. H. Sharp, Quart. Revs, 24 (1970) 185.
3. R. Pampuch, Proc. 9th Conf. Silicate Ind. Budapest, 1968, p. 143.
4. H. F. W. Taylor, Clay Min. Bull., 5 (1962) 45.
5. R. S. Gordon and W. D. Kingery, J. Amer. Ceram. Soc., 50 (1967) 8.
6. S. J. Gregg and R. I. Razouk, J. Chem. Soc. (1949) 536.
7. P. J. Anderson and R. F. Horlock, Trans. Farad. Soc., 58 (1962) 1993.
8. R. C. Turner, I. Hoffman and D. Chen, Can. J. Chem., 41 (1963) 243.
9. M. C. Ball and H. F. W. Taylor, Min. Mag., 32 (1961) 754.
10. N. H. Brett and P. J. Anderson. Trans. Farad. Soc., 63 (1967) 2044.
11. (a) H. Saalfeld and B. Behrota, Ber. Dtsch. Keram. Ges., 42 (1965) 161.
    (b) G. W. Brindley and J. O. Choe, Am. Min., 46 (1961) 771.
12. C. Eyraud and R. Goton, J. Chim. Phys., 51 (1954) 430.
13. G. W. Brindley and M. Nakahira, Z. Krist. 112 (1959) 136.
14. G. W. Brindley, J. H. Sharp, J. H. Patterson and B. N. N. Achar, Am. Min., 52 (1967) 201.
15. P. W. Clark and J. White, Trans. Brit. Ceram. Soc., 49 (1950) 305.
16. I. F. Guilliatt and N. H. Brett, J. Brit. Ceram. Soc., 6 (1969) 56.
17. F. W. Jones, Proc. Roy. Soc. (London), 166A (1938) 16.

18. A. S. RUSSELL, W. H. GITZEN, J. W. NEWSOME, R. W. RICKER, V. W. STOWE, H. C. STUMPF, J. R. WALL and P. WALLACE, Alumina Properties, Alcoa Res. Labs. Tech. Paper 10 (1956).
19. F. FREUND and H. GENTSCH, Ber. Dtsch. Keram. Ges., 44 (1967) 51.
20. J. J. FRIPIAT, H. BOSMANS and P. G. ROUXHET, J. Phys. Chem., 71 (1967) 1097.
21. P. G. ROUXHET, R. TOUILLEAUX, M. MESDAGH and J. J. FRIPIAT, Proc. Int. Clay Conf. Tokyo, 1 (1969) 109.
22. J. LAMING and J. WHITE, Personal communication.
23. C. ECKART, Phys. Rev., 35 (1930) 1303.
24. P. G. ROUXHET, Personal communication.

RÉSUMÉ — Etude thermogravimétrique de l'influence d'un champ électrique sur la déshydroxylation de $Mg(OH)_2$ (brucite) et de $Al(OH)_3$ (gibbsite) en atmosphère inerte contrôlée. L'application d'un champ électrique ne favorise pas la réaction de la gibbsite; parfois elle la retarde légèrement. Au contraire, un effet favorable faible mais significatif est observé avec la brucite où la température du début du phénomène ainsi que l'énergie d'activation sont abaissées sous l'effet de champs d'environ 10^5 V/m. On attribue la différence de comportement des deux hydroxydes aux différences de mobilité des défauts anioniques et des "complexes de transfert protonique" contenant de l'oxygène. On discute le phénomène de transport des différentes espèces porteurs de protons dans un champ électrique.

ZUSAMMENFASSUNG — Die Wirkung elektrischer Felder auf die thermische Dehydroxylierung von $Mg(OH)_2$ (Brucit) und $Al(OH)_3$ (Gibbsit) wurde mittels Thermogravimetrie in geregelter inerter Atmosphäre studiert. Die Gibbsit-Reaktion wird von elektrischen Feldern nicht gefördert; in manchen Fällen wird die Reaktion etwas verzögert. Beim Brucit hingegen kann eine geringe, doch signifikante Förderung beobachtet werden, indem die Anfangstemperatur und die Aktivierungsenergie bei Feldstärken von etwa 10^5 V/m herabgesetzt werden. Der Unterschied des Verhaltens der zwei Hydroxyde wird Unterschieden zwischen den Beweglichkeiten anionendefekter und sauerstoffhaltiger "Proton-Übertragungs-Komplexe" zugeschrieben. Der Transport der verschiedenen Protonenträger im elektrischen Feld wird erörtert.

Резюме. — Влияние электрического поля на термическое дегидроксилирование $Mg(OH)_2$ (бруцит) и $Al(OH)_3$ (гиббсит) изучено методом термогравиметрии в инертной атмосфере. Электрическое поле не оказывает положительного эффекта на реакцию гиббсита; в некоторых случаях реакция немного задерживается. В противоположность гиббситу небольшой эффект наблюдался для случая бруцита, для которого начальная температура и энергия активации снижаются при силе поля 10^5 V/м. Разница, обнаруженная в поведении этих двух гидроокисей, соответствует различной подвижности анионного дефекта и кислородсодержащих протон-переносных комплексов. Обсуждается переход различных протононесущих видов в электрическом поле.